

Article

Bifurcation and complex dynamics of a discrete-time predator–prey system

S. M. Sohel Rana

Department of Mathematics, University of Dhaka, Dhaka-1000, Bangladesh

E-mail: srana.mthdu@gmail.com

Received 22 December 2014; Accepted 10 February 2015; Published online 1 June 2015



Abstract

In this paper, we investigate the dynamics of a discrete-time predator-prey system of Holling-I type in the closed first quadrant R_+^2 . The existence and local stability of positive fixed point of the discrete dynamical system is analyzed algebraically. It is shown that the system undergoes a flip bifurcation and a Neimark-Sacker bifurcation in the interior of R_+^2 by using bifurcation theory. It has been found that the dynamical behavior of the model is very sensitive to the parameter values and the initial conditions. Numerical simulation results not only show the consistence with the theoretical analysis but also display the new and interesting dynamic behaviors, including phase portraits, period-9, 10, 20-orbits, attracting invariant circle, cascade of period-doubling bifurcation from period-20 leading to chaos, quasi-periodic orbits, and sudden disappearance of the chaotic dynamics and attracting chaotic set. In particular, we observe that when the prey is in chaotic dynamic, the predator can tend to extinction or to a stable equilibrium. The Lyapunov exponents are numerically computed to characterize the complexity of the dynamical behaviors. The analysis and results in this paper are interesting in mathematics and biology.

Keywords discrete-time predator-prey system; chaos; flip and Neimark-Sacker bifurcations; Lyapunov exponents.

Computational Ecology and Software
ISSN 2220-721X
URL: <http://www.iaees.org/publications/journals/ces/online-version.asp>
RSS: <http://www.iaees.org/publications/journals/ces/rss.xml>
E-mail: ces@iaees.org
Editor-in-Chief: Wenjun Zhang
Publisher: International Academy of Ecology and Environmental Sciences

1 Introduction

The dynamics of predator-prey interaction is the starting point for many variations that yield more realistic biological and mathematical problems in population ecology. Predation is a direct interaction which occurs when individuals from one population derive their nourishment by capturing and ingesting individuals from another population. There are many articles devoted to the study of predator-prey interaction both from the experimental and the modeling point of view. It is well known the Lotka-Volterra predator-prey model is one of the fundamental population models; a predator-prey interaction has been described firstly by two pioneers Lotka (1924) and Volterra (1926) in two independent works. After them, more realistic prey-predator model

were introduced by Holling suggesting three types of functional responses for different species to model the phenomena of predation (Holling, 1965).

Qualitative analyses of prey-predator models describe by set of differential equations were studied by many authors (Brauer and Castillo, 2001; Hastings and Powell, 1991; Klebanoff and Hastings, 1994; May, 1974; Murray, 1998; Zhu et al., 2002). Another possible way to understand a prey-predator interaction is by using discrete-time models. These models are more reasonable than the continuous time models when populations have non-overlapping generations (Brauer and Castillo, 2001; Murray, 1998) and lead to unpredictable dynamic behaviors from a biological point of view. This suggests the possibility that the governing laws of ecological systems may be relatively simple and therefore discoverable. The author (May, 1975, 1976) had clearly documented the rich array of dynamic behavior possible in simple discrete-time models. Recently, there is a growing evidence showing that the dynamics of the discrete-time prey-predator models can present a much richer set of patterns than those observed in continuous-time models (Agiza et al., 2009; Danca et al., 1997; Elsadany et al., 2012; Hasan et al., 2012; He and Lai, 2011; Jing and Yang, 2006; Li, 1975; Liu, 2007; Hu et al., 2011; He and Li, 2014). However, there are few articles discussing the dynamical behaviors of predator-prey models, which include bifurcations and chaos phenomena for the discrete-time models. The authors (He and Lai, 2011; Jing, 2006; Liu, 2007; Hu et al., 2011) obtained the flip bifurcation by using the center manifold theorem and bifurcation theory. But in (Agiza et al., 2009; Danca et al., 1997; Elsadany et al., 2012), the authors only showed the flip bifurcation and Hopf bifurcation by using numerical simulations. In this work, we confine our interest to present, by using both analytic and numerical methods, the domains of the values of the parameters under which the system predicts that the populations will be able to persist at a steady state, the conditions for flip and/or Neimark-Sacker bifurcations by using the normal form theory of the discrete system (see section 4, Kuznetsov, 1998) and the domain for the presence of chaos in the system by measuring the maximum Lyapunov exponents.

In ecology, many species have no overlap between successive generations, and thus their population evolves in discrete-time steps (Murray, 1998). Such a population dynamics is described by difference equation. Let x_n denotes the number of prey population and y_n the number of predator population in the n th generation. Our model is described by the following system of nonlinear difference equations in non-dimensional form:

$$H : \begin{cases} x_{n+1} = rx_n(1 - x_n) - ax_ny_n \\ y_{n+1} = bx_ny_n - dy_n \end{cases} \quad (1)$$

In the system (1), the prey grows logistically with intrinsic growth rate r and carrying capacity one in the absence of predation. The predator consumes the prey with functional response Holling type I. All parameters r, a, b, d have positive values that stand for prey intrinsic growth rate, per capita searching efficiency of the predator, conversion rate, and the death rate of the predator, respectively. From mathematical and biological point of view, we will pay attention on the dynamical behaviors of (1) in the closed first quadrant R_+^2 . Starting with initial population size (x_0, y_0) , the iteration of system (1) is uniquely determined a trajectory of the states of population output in the following form

$$(x_n, y_n) = H^n(x_0, y_0), \text{ where } n = 0, 1, 2, \dots$$

Our results in this paper are extension to those in (Danca et al., 1997; Elsadany et al., 2012). This paper is organized as follows. In Section 2, we discuss the existence and local stability of positive fixed point for system (1) in R_+^2 . In Section 3, we show that there exist some values of the parameters such that (1) undergoes the flip bifurcation and the Neimark-Sacker bifurcation in the interior of R_+^2 . In section 4, we present the numerical simulations which not only illustrate our results with theoretical analysis but also exhibit complex dynamical behaviors such as the cascade periodic-doubling bifurcation in periods 2, 4, 8, 9, 10, 20-orbits, quasi-periodic orbits and chaotic sets. Finally a short discussion is given in Section 5.

2 Existence and Local Stability of Fixed Points

In this section, we shall first discuss the existence of fixed points for (1), then study the stability of the fixed point by the eigenvalues for the Jacobian matrix of (1) at the fixed point. It is clear that the system (1) has the following fixed points in the (x, y) -plane:

$$E_0(0,0), E_1\left(\frac{r-1}{r}, 0\right) \text{ and } E_2(x^*, y^*), \text{ where } x^* = \frac{1+d}{b} \text{ and } y^* = \frac{r}{a}\left(1 - \frac{1+d}{b}\right) - \frac{1}{a}.$$

To discuss the existence of fixed points, we say that fixed points will not exist if any one of its components is negative. The fixed point E_0 always exists. The existence condition for E_1 is $r > 1$. Finally, the feasibility condition for the positive fixed point E_2 is

$$r > \frac{b}{b-1-d} \text{ (or } b > \frac{r(1+d)}{r-1}, r > 1).$$

Now we study the stability of the positive fixed point (we left the others) only. Note that the local stability of the fixed point (x, y) is determined by the modules of eigenvalues of the characteristic equation at the fixed point.

The Jacobian matrix due to the linearization of (1) evaluated at E_2 is given by

$$J(x^*, y^*) = \begin{pmatrix} 1 - \frac{(1+d)r}{b} & -\frac{a(1+d)}{b} \\ \frac{b(r-1) - (1+d)r}{a} & 1 \end{pmatrix}$$

and the characteristic equation of the Jacobian matrix J can be written as

$$\lambda^2 + \alpha_1\lambda + \alpha_2 = 0 \tag{2}$$

where $\alpha_1 = -trJ = -2 + \frac{(1+d)r}{b}$ and $\alpha_2 = \det J = (1+d)r\left(1 - \frac{2+d}{b}\right) - d$.

Therefore, the eigenvalues of J are

$$\lambda_{1,2} = -\frac{\alpha_1}{2} \pm \sqrt{\Delta} = 1 - \frac{(1+d)r}{2b} \pm \sqrt{\Delta} \tag{3}$$

where $\Delta = \left(\frac{\alpha_1}{2}\right)^2 - \alpha_2 = \left(1 + \frac{(1+d)r}{2b}\right)^2 - (1+d)r\left(1 - \frac{d}{b}\right) + d$.

Using Jury's criterion (Elaydi, 1996), we have necessary and sufficient condition for local stability of the fixed point E_2 which are given in the following proposition.

Proposition 1. When $r > \frac{b}{b-1-d}$, then system (1) has a positive fixed point E_2 and

(i) it is a sink if one of the following conditions holds:

$$(i.1) \quad \Delta \geq 0 \text{ and } \frac{(1+d)(3+d)r}{3-d+(1+d)r} < b < \frac{(2+d)r}{r-1};$$

$$(i.2) \quad \Delta < 0 \text{ and } b < \frac{(2+d)r}{r-1}.$$

(ii) it is a source if one of the following conditions holds:

$$(ii.1) \quad \Delta \geq 0 \text{ and } b > \max \left\{ \frac{(1+d)(3+d)r}{3-d+(1+d)r}, \frac{(2+d)r}{r-1} \right\};$$

$$(ii.2) \quad \Delta < 0 \text{ and } b > \frac{(2+d)r}{r-1}.$$

(iii) it is non-hyperbolic if one of the following conditions holds:

$$(iii.1) \quad \Delta \geq 0 \text{ and } b = \frac{(1+d)(3+d)r}{3-d+(1+d)r};$$

$$(iii.2) \quad \Delta < 0 \text{ and } b = \frac{(2+d)r}{r-1}.$$

(iv) it is a saddle for the other values of parameters except those values in (i)–(iii).

Following Jury's criterion, we can see that one of the eigenvalues of $J(E_2)$ is -1 and the others are neither 1 nor -1 if the term (iii.1) of Proposition 1 holds. Therefore, there may be flip bifurcation of the fixed point E_2 if r varies in the small neighborhood of FB_{E_2} where

$$FB_{E_2} = \left\{ (r, a, b, d) : r = \frac{b(-3+d)}{(1+d)(-3+b-d)}, \Delta \geq 0, r > 1, a, b, d > 0 \right\}.$$

Also when the term (iii.2) of Proposition 1 holds, we can obtain that the eigenvalues of $J(E_2)$ are a pair of conjugate complex numbers with module one. The conditions in the term (iii.2) of Proposition 1 can be written as the following set:

$$NS_{E_2} = \left\{ (r, a, b, d) : r = \frac{b}{-2+b-d}, \Delta < 0, r > 1, a, b, d > 0 \right\}$$

and if the parameter r varies in the small neighborhood of NS_{E_2} ; then the Neimark-Sacker bifurcation will appear.

3 Flip Bifurcation and Neimark-Sacker Bifurcation

In this section, we choose the parameter r as a bifurcation parameter to study the flip bifurcation and the Neimark-Sacker bifurcation of E_2 by using bifurcation theory in (see Section 4 in Kuznetsov, 1998; see also Guckenheimer and Holmes, 1983; Robinson, 1999; Wiggins, 2003).

We first discuss the flip bifurcation of (1) at E_2 . Suppose that $\Delta > 0$, i.e.,

$$\left(1 + \frac{(1+d)r}{2b}\right)^2 - (1+d)r\left(1 - \frac{d}{b}\right) + d > 0. \tag{4}$$

Let $r_1 = \frac{b(-3+d)}{(1+d)(-3+b-d)}$, then the eigenvalues of J are

$$\lambda_1(r_1) = -1, \text{ and } \lambda_2(r_1) = \frac{6-3b+4d}{3-b+d}.$$

The condition $|\lambda_2(r_1)| \neq 1$ leads to

$$\frac{6-3b+4d}{3-b+d} \neq \pm 1. \tag{5}$$

Let $\tilde{x} = x - x^*$, $\tilde{y} = y - y^*$ and $A(r) = J(x^*, y^*)$, we transform the fixed point (x^*, y^*) of system (1) into the origin, then system (1) becomes

$$\begin{pmatrix} \tilde{x} \\ \tilde{y} \end{pmatrix} \rightarrow A(r) \begin{pmatrix} \tilde{x} \\ \tilde{y} \end{pmatrix} + \begin{pmatrix} F_1(\tilde{x}, \tilde{y}, r) \\ F_2(\tilde{x}, \tilde{y}, r) \end{pmatrix} \tag{6}$$

where

$$\begin{aligned} F_1(\tilde{x}, \tilde{y}, r) &= -(r\tilde{x}^2 + a\tilde{x}\tilde{y}) + O(\|X\|^4), \\ F_2(\tilde{x}, \tilde{y}, r) &= b\tilde{x}\tilde{y} + O(\|X\|^4), \end{aligned} \tag{7}$$

and $X = (\tilde{x}, \tilde{y})^T$. It follows that

$$B_1(x, y) = \sum_{j,k=1}^2 \frac{\partial^2 F_1(\xi, r)}{\partial \xi_j \partial \xi_k} \Big|_{\xi=0} x_j y_k = -2rx_1 y_1 - ax_1 y_2 - ax_2 y_1,$$

$$B_2(x, y) = \sum_{j,k=1}^2 \frac{\partial^2 F_2(\xi, r)}{\partial \xi_j \partial \xi_k} \Big|_{\xi=0} x_j y_k = bx_1 y_2 + bx_2 y_1,$$

$$C_1(x, y, u) = \sum_{j,k,l=1}^2 \frac{\partial^3 F_1(\xi, r)}{\partial \xi_j \partial \xi_k \partial \xi_l} \Big|_{\xi=0} x_j y_k u_l = 0,$$

$$C_2(x, y, u) = \sum_{j,k,l=1}^2 \frac{\partial^3 F_2(\xi, r)}{\partial \xi_j \partial \xi_k \partial \xi_l} \Big|_{\xi=0} x_j y_k u_l = 0,$$

and $r = r_1$.

Therefore, $B(x, y) = \begin{pmatrix} B_1(x, y) \\ B_2(x, y) \end{pmatrix}$ and $C(x, y, u) = \begin{pmatrix} C_1(x, y, u) \\ C_2(x, y, u) \end{pmatrix}$ are symmetric multilinear vector functions of $x, y, u \in \mathbb{R}^2$.

We know that A has simple eigenvalue $\lambda_1(r_1) = -1$, and the corresponding eigenspace E^c is one-dimensional and spanned by an eigenvector $q \in \mathbb{R}^2$ such that $A(r_1)q = -q$. Let $p \in \mathbb{R}^2$ be the adjoint eigenvector, that is, $A^T(r_1)p = -p$. By direct calculation we obtain

$$\begin{aligned} q &\sim (-1 + d - bx^*, by^*)^T, \\ p &\sim (-1 + d - bx^*, -ay^*)^T. \end{aligned}$$

In order to normalize p with respect to q , we denote

$$p = \gamma_1 (-1 + d - bx^*, -ay^*)^T$$

where

$$\gamma_1 = \frac{1}{(-1 + d - bx^*)^2 - abx^*y^*}.$$

It is easy to see $\langle p, q \rangle = 1$, where $\langle \cdot, \cdot \rangle$ means the standard scalar product in \mathbb{R}^2 : $\langle p, q \rangle = p_1q_1 + p_2q_2$.

Following the algorithms given in (Kuznetsov, 1998), the sign of the critical normal form coefficient $\beta_1(r_1)$, which determines the direction of the flip bifurcation, is given by the following formula:

$$\beta_1(r_1) = \frac{1}{6} \langle p, C(q, q, q) \rangle - \frac{1}{2} \langle p, B(q, (A - I)^{-1} B(q, q)) \rangle \quad (8)$$

From the above analysis and the theorem in (Kuznetsov, 1998; Guckenheimer and Holmes, 1983; Robinson, 1999; Wiggins, 2003), we have the following result.

Theorem 1. Suppose that (x^*, y^*) is the positive fixed point. If the conditions (4), (5) hold and $\beta_1(r_1) \neq 0$, then system (1) undergoes a flip bifurcation at the fixed point (x^*, y^*) when the parameter r varies in a small neighborhood of r_1 . Moreover, if $\beta_1(r_1) > 0$ (respectively, $\beta_1(r_1) < 0$), then the period-2 orbits that bifurcate from (x^*, y^*) are stable (respectively, unstable).

In Section 4, we will give some values of the parameters such that $\beta_1(r_1) \neq 0$, thus the flip bifurcation occurs as r varies (see Figure 1).

We next discuss the existence of a Neimark-Sacker bifurcation by using the Neimark-Sacker theorem in (Kuznetsov, 1998; Guckenheimer and Holmes, 1983; Robinson, 1999; Wiggins, 2003).

It is clear that the eigenvalues $\lambda_{1,2}$ given by (3) are complex for $(trJ)^2 - 4 \det J < 0$, which leads to $\Delta < 0$, i.e.,

$$\left(1 + \frac{(1+d)r}{2b}\right)^2 - (1+d)r\left(1 - \frac{d}{b}\right) + d < 0 \tag{9}$$

Let $r_2 = \frac{b}{-2+b-d}$,

then we have $\det J(r_2) = 1$.

For $r = r_2$, the eigenvalues of the matrix associated with the linearization of the map (6) at $(x^*, y^*) = (0,0)$ are conjugate with modulus 1, and they are written as

$$\lambda_{1,2} = -\frac{\alpha_1(r_2)}{2} \pm \frac{i}{2}\sqrt{4\alpha_2(r_2) - \alpha_1^2(r_2)} \tag{10}$$

and $|\lambda_i(r_2)| = 1$, $\left. \frac{d|\lambda_i(r)|}{dr} \right|_{r=r_2} = \frac{(-2+b-d)(1+d)}{2b} \neq 0$, $i = 1,2$. Note that $\lambda_2 = \overline{\lambda_1}$.

In addition, if $\text{tr}J(r_2) \neq 0, -1$, which leads to

$$\frac{(1+d)r_2}{b} \neq 2,3,$$

then we have $\lambda_i^k(r_2) \neq 1$ for $k = 1,2,3,4$.

Let $q \in \mathbb{C}^2$ be an eigenvector of $A(r_2)$ corresponding to the eigenvalue $\lambda_1(r_2)$ such that

$$A(r_2)q = \lambda_1(r_2)q, \quad A(r_2)\bar{q} = \overline{\lambda_1(r_2)}\bar{q}.$$

Also let $p \in \mathbb{C}^2$ be an eigenvector of the transposed matrix $A^T(r_2)$ corresponding to its eigenvalue, that is, $\overline{\lambda_1(r_2)} = \lambda_2(r_2)$,

$$A^T(r_2)p = \lambda_2(r_2)p, \quad A^T(r_2)\bar{p} = \overline{\lambda_2(r_2)}\bar{p}.$$

By direct calculation we obtain

$$q \sim \left(\lambda_1 + d - bx^*, by^*\right)^T, \\ p \sim \left(\lambda_2 + d - bx^*, -ay^*\right)^T.$$

In order to normalize p with respect to q , we denote

$$p = \gamma_2 (\lambda_2 + d - bx^*, -ay^*)^T$$

where

$$\gamma_2 = \frac{1}{(\lambda_2 + d - bx^*)^2 - abx^*y^*}.$$

It is easy to see $\langle p, q \rangle = 1$, where $\langle \cdot, \cdot \rangle$ means the standard scalar product in \mathbb{C}^2 :
 $\langle p, q \rangle = \bar{p}_1 q_1 + \bar{p}_2 q_2$.

Any vector $X \in \mathbb{R}^2$ can be represented for r near r_2 as $X = zq + \bar{z}\bar{q}$, for some complex z . Indeed, the explicit formula to determine z is $z = \langle p, X \rangle$. Thus, system (6) can be transformed for sufficiently small $|r - r_2|$ (near r_2) into the following form:

$$z \mapsto \lambda_1(r)z + g(z, \bar{z}, r),$$

where $\lambda_1(r)$ can be written as $\lambda_1(r) = (1 + \varphi(r))e^{i\theta(r)}$ (where $\varphi(r)$ is a smooth function with $\varphi(r_2) = 0$) and g is a complex-valued smooth function of z, \bar{z} , and r , whose Taylor expression with respect to (z, \bar{z}) contains quadratic and higher-order terms:

$$g(z, \bar{z}, r) = \sum_{k+l \geq 2} \frac{1}{k!l!} g_{kl}(r) z^k \bar{z}^l, \text{ with } g_{kl} \in \mathbb{C}, k, l = 0, 1, \dots$$

By symmetric multilinear vector functions, the Taylor coefficients g_{kl} can be expressed by the formulas

$$\begin{aligned} g_{20}(r_2) &= \langle p, B(q, q) \rangle, & g_{11}(r_2) &= \langle p, B(q, \bar{q}) \rangle, \\ g_{02}(r_2) &= \langle p, B(\bar{q}, \bar{q}) \rangle, & g_{21}(r_2) &= \langle p, C(q, q, \bar{q}) \rangle, \end{aligned}$$

and the coefficient $\beta_2(r_2)$, which determines the direction of the appearance of the invariant curve in a generic system exhibiting the Neimark-Sacker bifurcation, can be computed via

$$\beta_2(r_2) = \operatorname{Re} \left(\frac{e^{-i\theta(r_2)} g_{21}}{2} \right) - \operatorname{Re} \left(\frac{(1 - 2e^{i\theta(r_2)})e^{-2i\theta(r_2)}}{2(1 - e^{i\theta(r_2)})} g_{20} g_{11} \right) - \frac{1}{2} |g_{11}|^2 - \frac{1}{4} |g_{02}|^2,$$

where $e^{i\theta(r_2)} = \lambda_1(r_2)$.

For the above argument and the theorem in (Kuznetsov, 1998; Guckenheimer and Holmes, 1983; Robinson, 1999; Wiggins, 2003), we have the following result.

Theorem 2. Suppose that (x^*, y^*) is the positive fixed point. If $\beta_2(r_2) < 0$ (respectively, > 0) the Neimark-Sacker bifurcation of system (1) at $r = r_2$ is supercritical (respectively, subcritical) and there exists a unique closed invariant curve bifurcation from (x^*, y^*) for $r = r_2$, which is asymptotically stable (respectively, unstable).

In Section 4 we will choose some values of the parameters so as to show the process of a Neimark-Sacker

bifurcation for system (1) in Figure 2 by numerical simulation.

4 Numerical Simulations

In this section, our aim is to present numerical simulations to explain the above theoretical analysis, especially the bifurcation diagrams, phase portraits and Maximum Lyapunov exponents for system (1) around the positive fixed point E_2 and show the new interesting complex dynamical behaviors. It is known that Maximum Lyapunov exponents quantify the exponential divergence of initially close state-space trajectories and frequently employ to identify a chaotic behaviour. We choose the growth rate of prey, r as the real bifurcation parameter (varied parameter) and other model parameters are as fixed parameters, otherwise stated. For showing the dynamics of the system (1) change, the bifurcation parameters are considered in the following cases:

Case (i): varying r in range $3 \leq r \leq 4$, and $a = 3, b = 1.95, d = 0.25$ fixing.

Case (ii): varying r in range $1 \leq r \leq 2.97$, and $a = 3.5, b = 4.5, d = 0.25$ fixing.

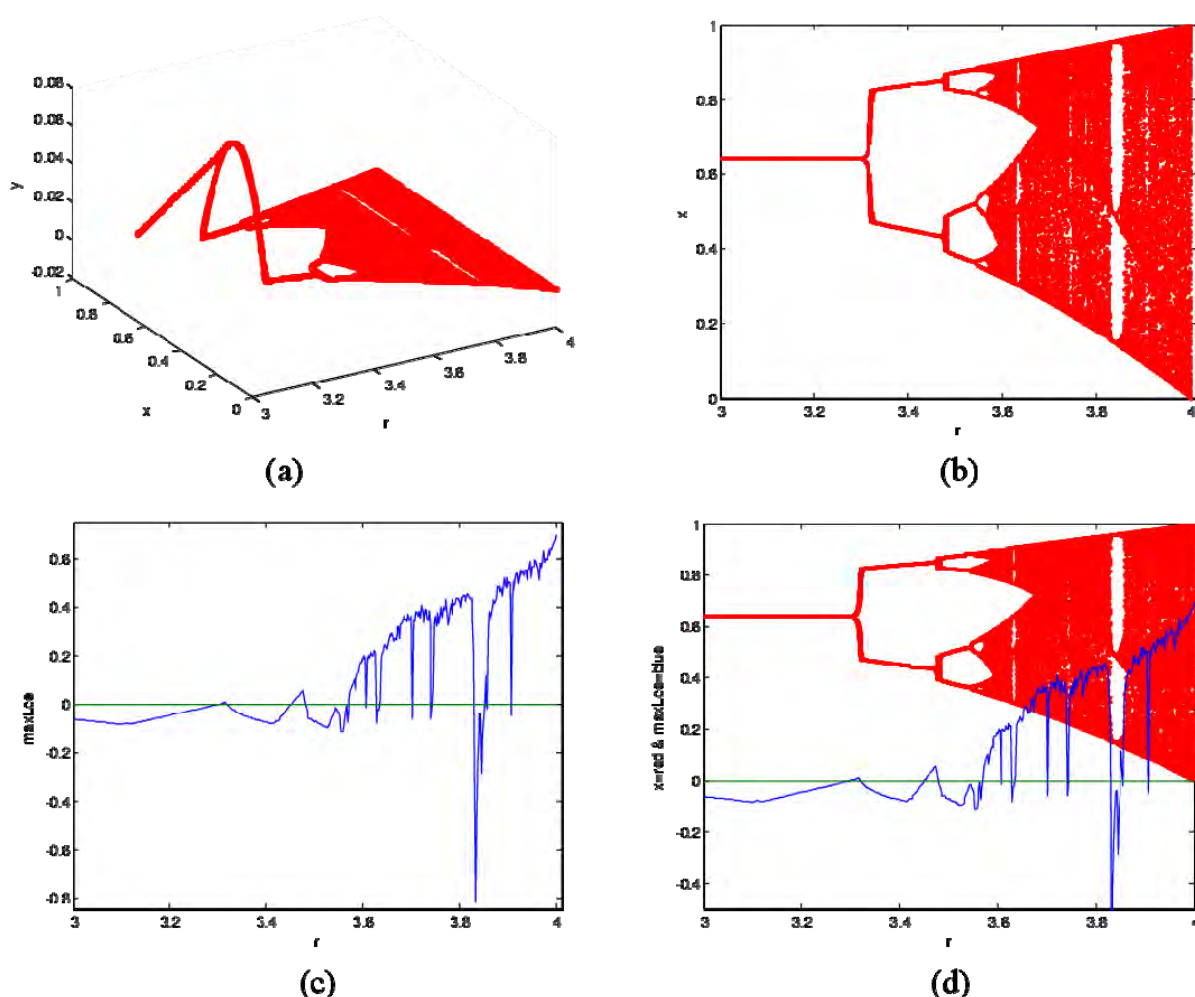


Fig. 1 Bifurcation diagrams and maximum Lyapunov exponent for system (1) around E_2 . (a) Flip bifurcation diagram of system (1) in $(r - x - y)$ space, the initial value is $(x_0, y_0) = (0.641, 0.061)$ (b) Flip bifurcation diagram in $(r - x)$ plane (c) Maximum Lyapunov exponents corresponding to (b) and (d) Maximum Lyapunov exponents are superimposed on Flip bifurcation diagram.

For case (i). The bifurcation diagrams of system (1) in $(r-x-y)$ space and in $(r-x)$ plane are given in Fig. 1(a-b). After calculation for the fixed point E_2 of map (1), the flip bifurcation emerges from the fixed point $(0.641, 0.062)$ at $r = r_1 = 3.3$ and $(a, b, d) \in FB_{E_2}$. It shows the correctness of proposition 1. At $r = r_1$, we have $\beta_1(r_1) = -14.167$, which determines the direction of the flip bifurcation and shows the correctness of Theorem 1. From Fig. 1(b), we see that the fixed point E_2 is stable for $r < 3.3$ and loses its stability at the flip bifurcation parameter value $r = 3.3$, we also observe that there is a cascade of period doubling bifurcations for $r > 3.3$. The maximum Lyapunov exponents corresponding to Fig. 1(b) are computed and plotted in Fig. 1(c), confirming the existence of the chaotic regions and period orbits in the parametric space.

For case (ii). The bifurcation diagrams of system (1) in the $(r-x-y)$ space, the $(r-x)$ plane and the $(r-y)$ plane are given in Fig. 2(a-b-c). After calculation for the fixed point E_2 of map (1), the Neimark-Sacker bifurcation emerges from the fixed point $(0.2778, 0.127)$ at $r = r_2 = 2$ and $(a, b, d) \in NS_{E_2}$. It shows the correctness of proposition 1. For $r = r_2$, we have $\lambda_{1,2} = 0.722222 \pm 0.691661 i$, $|\lambda_{1,2}| = 1$,

$$\left. \frac{d|\lambda_i(r)|}{dr} \right|_{r=r_2} = 0.3125 > 0, \quad g_{20} = -0.88889 + 1.65106 i, \quad g_{02} = -1.61111 - 4.57389 i,$$

$g_{11} = -1.25 + 1.30523 i$, $g_{21} = 0$, and $\beta_2(r_2) = -5.625$. Therefore, the Neimark-Sacker bifurcation is supercritical and it shows the correctness of Theorem 2.

From Fig. 2(b-c), we observe that the fixed point E_2 of map (1) is stable for $r < 2$ and loses its stability at $r = 2$ and an invariant circle appears when the parameter r exceeds 2, we also observe that there are period-doubling phenomenons. The maximum Lyapunov exponents corresponding to Fig. 2(b-c) are computed and plotted in Fig. 2(d), confirming the existence of the chaotic regions and period orbits in the parametric space. From Fig. 2(d), we observe that some Lyapunov exponents are bigger than 0, some are smaller than 0, so there exist stable fixed points or stable period windows in the chaotic region. In general the positive Lyapunov exponent is considered to be one of the characteristics implying the existence of chaos. The bifurcation diagrams for x and y together with maximum Lyapunov exponents is presented in Fig. 2(e). Fig. 2(f) is the local amplification corresponding to Fig. 2(b) for $r \in [2.7, 2.948]$.

The phase portraits which are associated with Fig. 2(a) are disposed in Fig. 3, which clearly depicts the process of how a smooth invariant circle bifurcates from the stable fixed point $(0.2778, 0.127)$. When r exceeds 2 there appears a circular curve enclosing the fixed point E_2 , and its radius becomes larger with respect to the growth of r . When r increases at certain values, for example, at $r = 2.745$, the circle disappears and a period-9 orbits appears, and some cascades of period doubling bifurcations lead to chaos. From Fig. 3, we observe that as r increases there are period-9, 10, 20-orbits, quasi-periodic orbits and attracting chaotic sets. See that for $r = 2.95$ & 2.97 , where the system is chaotic, is the value of maximal Lyapunov exponent positive that confirm the existence of the chaotic sets.

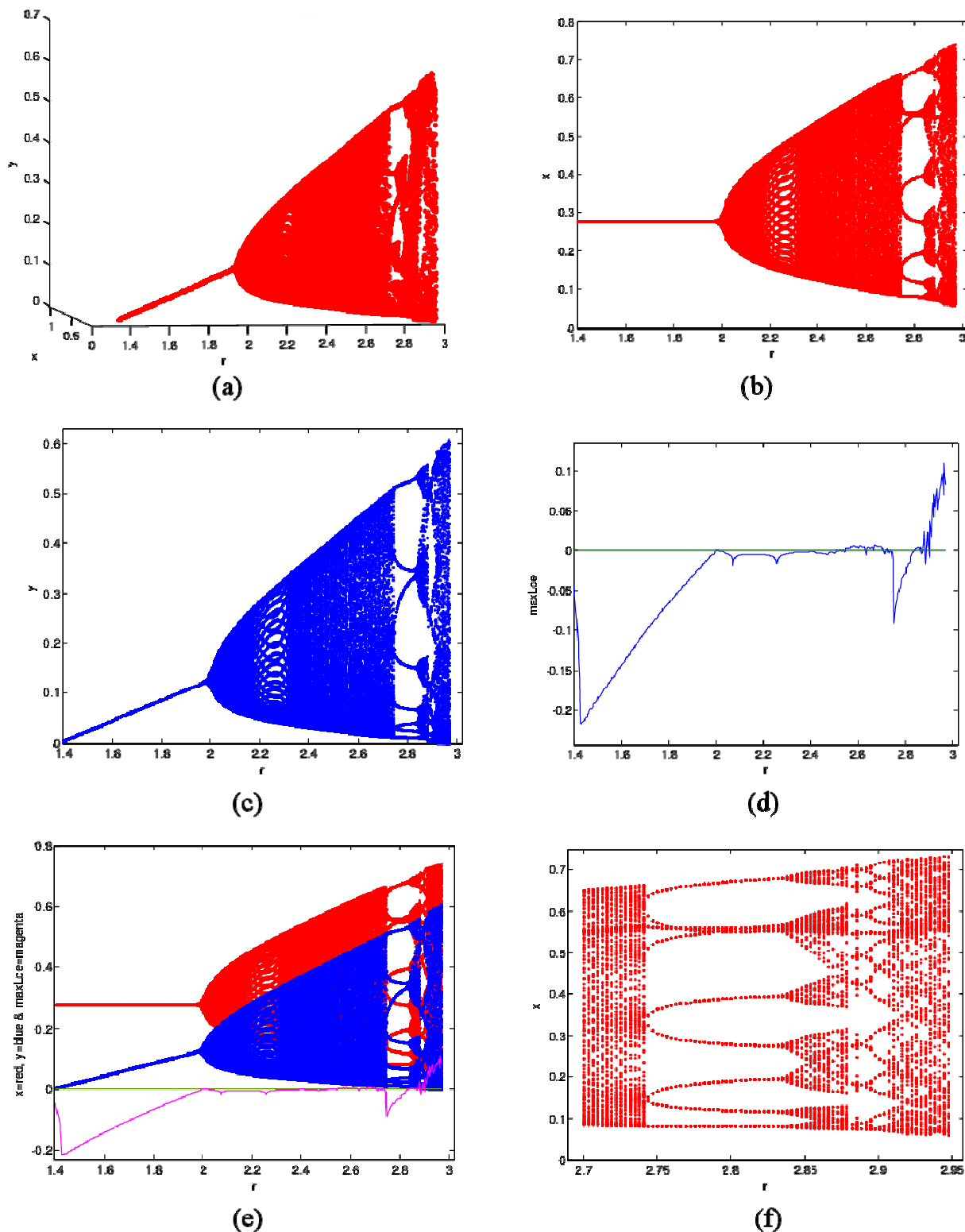


Fig. 2 Bifurcation diagrams and maximum Lyapunov exponent for system (1) around E_2 . (a) Neimark-Sacker bifurcation diagram of system (1) in $(r-x-y)$ space (b-c) Hopf bifurcation diagrams in $(r-x)$ and $(r-y)$ planes (d) Maximum Lyapunov exponents corresponding to (b-c) (e) Maximum Lyapunov exponents are superimposed on bifurcation diagrams (f) Local amplification corresponding to (a) for $r \in [2.7, 2.948]$. The initial value is $(x_0, y_0) = (0.25, 0.11)$.

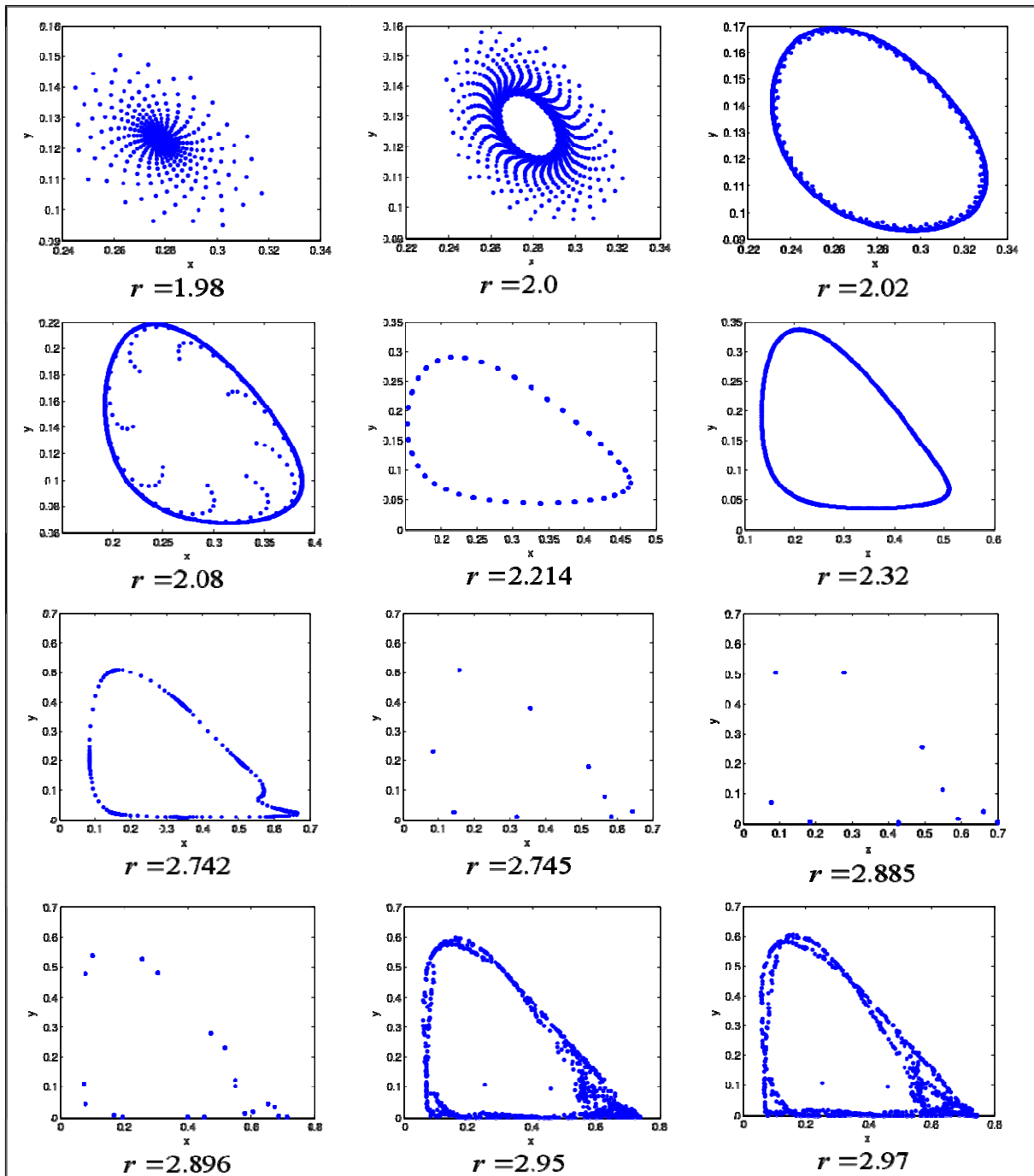


Fig. 3 Phase portraits for various values of r corresponding to Fig. 3(a).

In order to observe the complex dynamics, we can vary one more parameters of system (1). Since the values of Lyapunov exponents quantify the chaotic behavior of discrete system or at least sensitive dependence on initial conditions, so we compute maximum Lyapunov exponents of system (1) and study the dependence of these Lyapunov exponents on two real parameters r and b . The maximum Lyapunov exponents of system (1) for parameters $r \in [1.0, 2.97]$ and $b \in [2.5, 4.5]$ and fixing other parameters as in case (ii) is given in Fig. 4(a). In Fig. 4(b) is plotted the sign of the maximal Lyapunov exponent of map (1). Blue color represents negative Lyapunov exponent and red color represents positive Lyapunov exponent. Here it is easy to see for which choice of parameters the system (1) is showing chaotic motion, and for which one is the system (1)

exhibiting periodic or quasi periodic movement. E.g., the chaotic situation is on Fig. 3 for values of parameters $r = 2.97$ & $b = 4.5$ and the non-chaotic situation is for values of parameters $r = 2.745$ & $b = 4.5$ which are consistent with signs in Fig. 4(b).

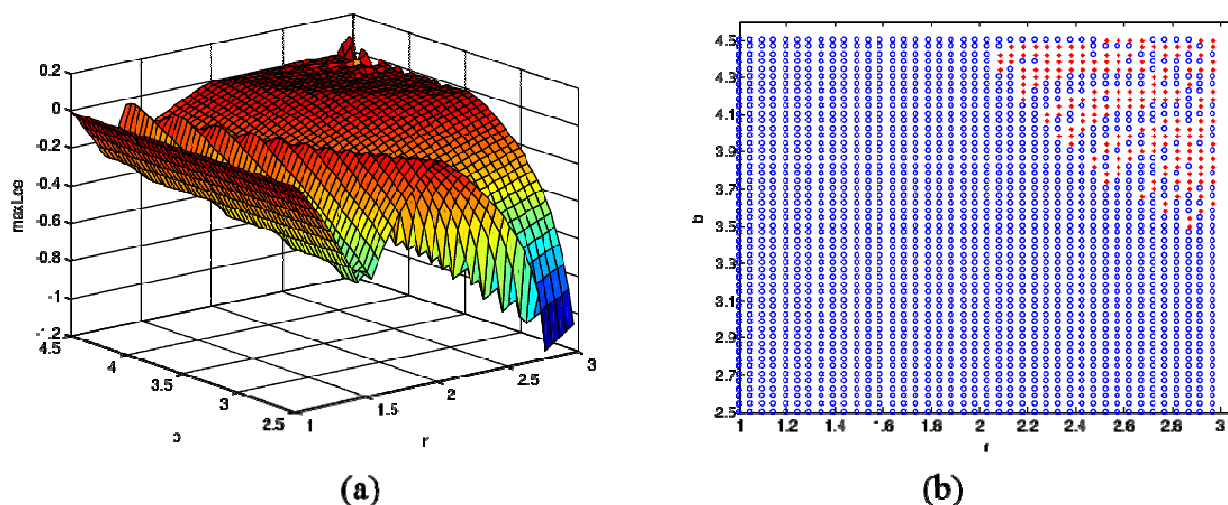


Fig. 4 Sign of maximum Lyapunov exponent for system (1) around E_2 . (a) Maximum Lyapunov exponents of system (1) covering $r \in [1.0, 2.97]$ and $b \in [2.5, 4.5]$ (b) Sign of Maximum Lyapunov exponents corresponding to (a) (red '*' = positive, blue 'o' = negative). The initial value is $(x_0, y_0) = (0.25, 0.11)$.

5 Discussion

In this paper, We performed a detailed computational analysis of the discrete-time predator-prey system (1) of Holling type I functional response and showed that it has a complex dynamics in the closed first quadrant R_+^2 . As certain parameters increase or decrease further away, we showed that system (1) can undergo a flip bifurcation and a Neimark-Sacker bifurcation in the interior of R_+^2 . Moreover, system (1) displayed much interesting dynamical behaviors, including period-9, 10, 20-orbits, invariant cycle, cascade of period-doubling, quasi-periodic orbits and the chaotic sets, which imply that the predators and prey can coexist in the stable period-n orbits and invariant cycle. Finally, simulation works showed that in certain regions of the parameter space, the model (1) had a great sensitivity to the choice of initial conditions and parameter values.

References

- Agiza HN, Elabbasy EM, EL-Metwally H, et al. 2009. Chaotic dynamics of a discrete prey-predator model with Holling type II. *Nonlinear Analysis: Real World Applications*, 10: 116-129
- Brauer F, Castillo-Chavez C. 2001. *Mathematical Models in Population Biology and Epidemiology*. Springer-Verlag, New York, USA
- Danca M, Codreanu S, Bako B. 1997. Detailed analysis of a nonlinear prey-predator model. *Journal of Biological Physics*, 23: 11-20
- Elaydi SN. 1996. *An Introduction to Difference Equations*. Springer-Verlag, USA
- Elsadany AA, EL-Metwally HA, Elabbasy EM, Agiza HN. 2012. Chaos and bifurcation of a nonlinear discrete

- prey-predator system. *Computational Ecology and Software*, 2(3): 169-180
- Guckenheimer J, Holmes P. 1983. *Nonlinear Oscillations, Dynamical Systems, and Bifurcations of Vector Fields*. Springer, New York, USA
- Hasan KA, Hama, M. F. 2012. Complex Dynamics Behaviors of a Discrete Prey-Predator Model with Beddington-DeAngelis Functional Response. *International Journal of Contemporary Mathematical Sciences*, 7(45): 2179-2195
- Hastings A, Powell T. 1991. Chaos in three-species food chain. *Ecology*, 72: 896-903
- He ZM, Lai X. 2011. Bifurcations and chaotic behavior of a discrete-time predator-prey system. *Nonlinear Analysis: Real World Applications*, 12: 403-417
- He ZM, Li Bo. 2014. Complex dynamic behavior of a discrete-time predator-prey system of Holling-III type. *Advances in Difference Equations*, 180
- Hu ZY, Teng Z, Zhang L. 2011. Stability and bifurcation analysis of a discrete predator-prey model with nonmonotonic functional response. *Nonlinear Analysis*, 12: 2356-2377
- Holling CS. 1965. The functional response of predator to prey density and its role in mimicry and population regulation. *Memoirs of the Entomological Society of Canada*, 45: 1-60
- Jing ZJ, Yang J. 2006. Bifurcation and chaos discrete-time predator-prey system. *Chaos, Solutions and Fractals*, 27: 259-277
- Klebanoff A, Hastings A. 1994. Chaos in three species food-chain. *Journal of Mathematical Biology*, 32: 427-245
- Kuznetsov YK. 1998. *Elements of Applied Bifurcation Theory* (3rd edn). Springer, New York, USA
- Li TY, Yorke JA. 1975. Period three implies chaos. *American Mathematical Monthly*, 82: 985-992
- Liu X, Xiao DM. 2007. Complex dynamic behaviors of a discrete-time predator prey system. *Chaos, Solutions and Fractals*, 32: 80-94
- Lotka AJ. 1925. *Elements of Mathematical Biology*, Williams and Wilkins, Baltimore, USA
- May RM. 1974. *Stability and Complexity in Model Ecosystems*. Princeton University Press, NJ, USA
- May RM. 1975. Biological populations obeying difference equations: stable points, stable cycles and chaos. *Journal of Theoretical Biology*, 51(2): 511-524
- May RM. 1976. Simple mathematical models with very complicated dynamics. *Nature*; 261:459-467
- Murray JD. 1998. *Mathematical Biology*. Springer-Verlag, Berlin, Germany
- Robinson C. 1999. *Dynamical Systems, Stability, Symbolic Dynamics and Chaos* (2nd edn). CRC Press, Boca Raton, USA
- Volterra V. 1926. *Variazioni e fluttuazioni del numero d'individui in specie animali conviventi*, Mem. R. Accad. Naz. Dei Lincei, Ser. VI, vol. 2
- Wiggins S. 2003. *Introduction to Applied Nonlinear Dynamical Systems and Chaos* (2nd edn). Springer, New York, USA
- Zhu H, Campbell SA, Wolkowicz G. 2002. Bifurcation analysis of a predator-prey system with nonmonotonic functional response. *SIAM Journal on Applied Mathematics*, 63: 636-682